

Transport properties of single atoms.

Alexei Bagrets¹, Nikos Papanikolaou², and Ingrid Mertig¹

¹*Martin-Luther-Universität Halle-Wittenberg, Fachbereich Physik, D-06099 Halle, Germany*

²*Institute of Microelectronics, NCSR "Demokritos", GR-15310 Athens, Greece*

(Dated: June 28, 2018)

We present a systematic study of the ballistic electron conductance through *sp* and *3d* transition metal atoms attached to copper and palladium crystalline electrodes. We employ the *ab initio* screened Korrington-Kohn-Rostoker Green's function method to calculate the electronic structure of nanocontacts while the ballistic transmission and conductance eigenchannels were obtained by means of the Kubo approach as formulated by Baranger and Stone. We demonstrate that the conductance of the systems is mainly determined by the electronic properties of the atom bridging the macroscopic leads. We classify the conducting eigenchannels according to the atomic orbitals of the contact atom and the irreducible representations of the symmetry point group of the system that leads to the microscopic understanding of the conductance. We show that if impurity resonances in the density of states of the contact atom appear at the Fermi energy, additional channels of appropriate symmetry could open. On the other hand the transmission of the existing channels could be blocked by impurity scattering.

PACS numbers: 73.63.Rt, 73.23.Ad, 75.47.Jn, 73.40.Cg

I. INTRODUCTION

State-of-the-art experimental techniques, like scanning tunneling microscopy (STM)¹ and mechanically controllable break junctions (MCBJ),^{2,3} enable the manipulation of individual atoms and the fabrication of metallic, atomic-sized contacts. From a fundamental scientific point of view these systems allow us to investigate a variety of phenomena at the ultimate limit of atomic scale and prove basic ideas of quantum mechanics. For example, when studying conductance, the familiar Ohm's law completely breaks down and the fully quantum-mechanical description should be applied to elucidate the phenomenon.^{4,5,6,7,8,9}

Our understanding of ballistic transport of atomic-sized conductors is usually based on the Landauer formula,¹⁰

$$G = \frac{2e^2}{h} \sum_{n=1}^N T_n,$$

where conductance is represented as a sum of transmission probabilities T_n of individual eigenchannels. When the T_n 's are known many properties of a system can be predicted such as conductance fluctuations,¹¹ the shot noise,¹² dynamical Coulomb blockade¹³ and the supercurrent.¹⁴ It has been demonstrated in the pioneering work by Scheer *et al.*¹⁵ that a study of the current-voltage characteristics for the superconducting atomic-sized contacts allows to obtain transmission probabilities T_n 's for particular atomic configurations realized in the MCBJ experiments. The T_n 's can be determined by fitting theoretical and experimental $I - V$ curves and exploiting information contained in the "sub-gap structure".^{15,16} The breakthrough in the interpretation of experimental results was done by Cuevas *et al.*⁶ who suggested a parameterized tight-binding model for

the description of atomic constrictions. As a central result it has been shown that the number of conducting modes (eigenchannels) for a single-atomic contact correlates with the number of valence orbitals of the contact atom which therefore determines the current flowing through the system. This result has been confirmed experimentally by Scheer *et al.*¹⁶ The analysis of the last conductance plateau corresponding to single-atom constrictions has revealed that a number of conducting channels is 1 for Au, 3 for Al and Pb, and 5 for Nb.

The main goal of this paper is to clarify with the help of parameter-free *ab initio* calculations the issue on how the valence states of the central atom of a single-atom contact determine conducting channels. Our approach is based on the screened Korrington-Kohn-Rostoker (KKR) Green's function method¹⁷ supplemented with the Baranger and Stone¹⁸ formulation of the conductance problem. Instead of considering a variety of different metallic atomic point contacts we restrict our calculations to single *sp* or *3d* transition metal atoms attached to noble metal (Cu) or transition metal (Pd) leads. Systems of this type can be realized experimentally by using alloys to fabricate the point contacts.^{19,20} According to our preliminary study,²¹ we await the variation of conductance depending on the atomic number of the impurity situated at the central site. The number of conducting modes is also expected to change with respect to the atomic number of the impurity, especially because of the existence of the virtual bound states. We would like to mention, that the conductance through different type of constrictions contaminated by impurities has been studied before on the *ab initio* level by Lang²², Hirose and coworkers²³ and Palotás and coworkers.²⁴ In contrast to previous studies, we analyze the eigenchannel decomposition of the conductance. Within our approach each channel is classified according to the irreducible representation of the corresponding point group of the system as well as by

orbital contributions when the channel wave function is projected on the central atom. That relates the method presented here with the tight-binding model suggested by Cuevas *et al.*⁶ and gives a microscopic insight into the conductance.

II. THEORETICAL APPROACH

A. Set-up of the problem

The structures under study consist of two semi-infinite Cu or Pd fcc (001) leads connected by an atomic cluster with a single contact atom in the middle of a junction as it is shown in Fig.1. We consider the contact atom to be either a host atom or different *sp* or *3d* transition metal impurities as will be discussed later. We assume that the geometry of constrictions shown in Fig.1 catches limiting configurations of atomic contacts produced in the MCBJ experiments. To realize different contact atoms one could use dilute alloys as a wire material in the MCBJ,^{19,20} or probe conductance through a single atom with an STM tip.²⁵ Since in the experiments the measurements are not performed for the equilibrium atomic configurations rather than the conductance is recorded dynamically under stretching of nanocontacts,³ we did not optimize the interatomic distances and kept them the same as in bulk fcc metals Cu and Pd with lattice constants 6.83 a.u. and 7.35 a.u., respectively.

B. Electronic structure calculation of atomic contacts

Our calculations are based on density functional theory within the local density approximation. We employed the non-relativistic version of the screened Korringa-Kohn-Rostoker (KKR) Green's function method to calculate the electronic structure of the systems. Since details of the method can be found elsewhere,²⁶ only a brief description is given below. The parametrization of Vosko, Wilk, and Nusair²⁷ for the exchange and correlation energy was used. The potentials were assumed to be spherically symmetric around each atom (atomic sphere approximation, ASA). However, the full charge density, rather than its spherically symmetric part, was taken into account. To achieve well converged results the angular momentum cut-off for the wavefunctions and the Green's function was chosen to be $l_{\max} = 3$ that imposed a natural cut-off $2l_{\max} = 6$ for the charge density expansion. In case of the heavy element Pd the scalar relativistic approximation²⁸ was used.

In the multiple-scattering KKR approach the one-electron retarded Green's function is given by the site

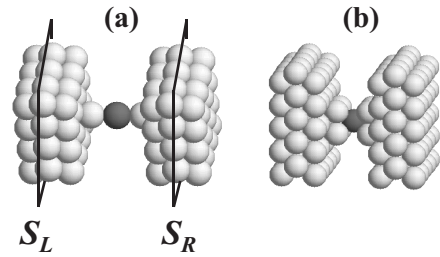


FIG. 1: Geometry of Cu and Pd atomic-sized constrictions studied in the paper: (a) three atom chain suspended between the leads; (b) pyramid-like contact. The central (contact) atom of the constriction can be either a host or impurity atom. The conductance is calculated between left (S_L) and right (S_R) planes positioned in the leads.

angular momentum expansion

$$\begin{aligned}
 G^+(\mathbf{R}_n + \mathbf{r}, \mathbf{R}_{n'} + \mathbf{r}'; E) &= \delta_{nn'} \sqrt{E} \sum_L R_L^n(\mathbf{r}_<; E) H_L^n(\mathbf{r}_>; E) \\
 &+ \sum_{LL'} R_L^n(\mathbf{r}; E) G_{LL'}^{nn'}(E) R_{L'}^{n'}(\mathbf{r}'; E)
 \end{aligned} \quad (1)$$

where \mathbf{r} , \mathbf{r}' are restricted to the cells n and n' ; $\mathbf{r}_<$, $\mathbf{r}_>$ denote one of the two vectors \mathbf{r} or \mathbf{r}' with the smaller or the larger absolute value, and local functions $R_L^n(\mathbf{r}; E)$ and $H_L^n(\mathbf{r}; E)$ are the regular and irregular solutions of the Schrödinger equation for the single potential $V_n(\mathbf{r})$ of the n -th cell in free space. Here the index $L = (l, m)$ stands for the angular momentum quantum numbers and atomic units are used: $e = -\sqrt{2}$, $\hbar = 1$, $m = 1/2$. The structural Green's function $G_{LL'}^{nn'}(E)$ (structure constants) in Eq. (1) is related to the known structure constants of the appropriately chosen reference system by the algebraic Dyson equation which includes the difference $\Delta t = \delta_{nn'} \delta_{LL'} \Delta t_L^n$ between local t -matrices of the physical and a reference system. In the screened KKR method¹⁷ we use a lattice of strongly repulsive, constant muffin-tin potentials (typically, $\sim 4\text{Ry}$ height) as reference system that leads to structure constants which decay exponentially in real space.

When the KKR method is applied to the systems shown in Fig.1 both the constriction region and the leads are treated on the same footing. This is achieved by using the hierarchy of Green's functions connected by a Dyson equation, so that one performs the self-consistent electronic structure calculations of complicated systems in a step-like manner. First, using the concept of principal layers together with the decimation technique,²⁹ we calculate the structural Green's function $G_{LL'}^{0jj'}(\mathbf{k}_\parallel, E)$ of the auxiliary system consisting of semi-infinite leads separated by a vacuum barrier (here j and j' refer to layer indexes). At the second step the atomic cluster is embedded between the leads by solving the Dyson equation

self-consistently,

$$G_{LL'}^{nn'}(E) = G_{LL'}^{0nn'}(E) + \sum_{n''L''} G_{LL''}^{0nn''}(E) \Delta t_{L''}^{n''}(E) G_{L''L'}^{n''n'}(E), \quad (2)$$

and the structural Green's function $G_{LL'}^{nn'}(E)$ of the complete system is obtained. Eq. (2) is solved in real space since due to effective screening of the perturbation the charge deviations are restricted nearby the constriction.

C. Evaluation of conductance

In what follows, we will consider only a ballistic coherent regime of the electron transport thus limiting our study to zero temperature, infinitely small bias and single-particle picture. To evaluate the conductance of nanocontacts we employ the Kubo linear response theory as formulated by Baranger and Stone:¹⁸

$$g = G_0 \int_{S_L} dS \int_{S_R} dS' \times G^+(\mathbf{r}, \mathbf{r}', E_F) \overset{\leftrightarrow}{\partial}_z \overset{\leftrightarrow}{\partial}_{z'} G^-(\mathbf{r}', \mathbf{r}, E_F), \quad (3)$$

here $G_0 = 2e^2/h$, G^- and G^+ are retarded and advanced Green's functions, respectively. The current flows in z direction, and $f \overset{\leftrightarrow}{\partial}_z g = f(\partial_z g) - (\partial_z f)g$. The integration is performed over two (left and right) planes S_L and S_R which connect the leads with the scattering region as it is shown in Fig. 1. The implementation of the Eq. (3) in the site angular momentum representation of the KKR method and related to its convergence properties were described in detail in Ref. 30. Within the ASA used in this work instead of integration over planes we average conductance over atomic layers and obtain:

$$g = G_0 \text{Tr}_{(n,L)} [D_L G D_R G^\dagger]. \quad (4)$$

Here, Tr involves site (n) and angular momentum (L) indices related to the atomic plane S_L (Fig. 1). $G = \{G_{LL'}^{nn'}(E_F)\}$ stands for the matrix notation of the structural Green's function introduced in Eq. (1), taken at the Fermi energy. Site-diagonal operators D_L and D_R related to the left (L) and right (R) leads are defined as

$$[D_{L(R)}]_{LL'}^{nn'} = \pm \frac{\delta_{nn'}}{\Delta} \int_{V_{L(R)}^n} d^3r \left[R_L^{n*}(\mathbf{r}, E_F) i \overset{\leftrightarrow}{\partial}_z R_L^n(\mathbf{r}, E_F) \right], \quad (5)$$

where different signs, "+" and "-", refer to different operators, D_L and D_R , respectively. The integral is performed over the volume $V_{L(R)}^n$ of the Wigner-Seitz cell around site n which belongs either to the atomic plane S_L or to the plane S_R , and Δ is the distance separating nearest-neighbor atomic layers in z direction.

D. Conductance eigenchannels

Ballistic conductance of an atomic constriction can be decomposed into individual eigenchannels. According to the Landauer formalism, which was proved to be equivalent to the Kubo approach,¹⁸ conductance reads as $g = G_0 \sum_n \tau_n(E_F)$. The τ_n 's are eigenvalues of the matrix $T_{\mathbf{k}\mu; \mathbf{k}'\mu'}$ which defines the transmission probability for an incident Bloch wave from the left electrode to be transmitted to an outgoing Bloch wave in the right, where \mathbf{k} and \mathbf{k}' are Bloch vectors for incident and transmitted waves, and μ and μ' are the corresponding band indices. A procedure for the evaluation of the conductance eigenchannels will be published elsewhere.³¹ To solve the eigenvalue problem for the transmission matrix T , the perturbed Bloch states of the whole system are projected to the basis of local functions $R_L^n(\mathbf{r})$ and conductance is represented as a sum of two contributions:

$$g = G_0 \text{Tr}_{(n,L)} [\mathcal{T}^+] + G_0 \text{Tr}_{(n,L)} [\mathcal{T}^-], \quad (6)$$

with

$$\mathcal{T}^\pm = \pm \sqrt{\pm D_L^\pm} G D_R G^\dagger \sqrt{\pm D_L^\pm}. \quad (7)$$

Here D_L^\pm are two parts of the anti-symmetric hermitian operator $D_L = D_L^+ + D_L^-$ defined by Eq.(5). The D_L^+ and D_L^- have positive and negative eigenvalues, respectively.

When the atomic plane S_L is placed in the asymptotic region of the left lead far from the atomic constriction the second term in Eq.(6), involving trace of \mathcal{T}^- , is equal to zero and eigenchannels are found as eigenvectors of operator \mathcal{T}^+ . However, in practice we are forced to take integration planes closer to the constriction in order to obtain convergent value for the conductance with respect to number of atoms in the cross-sections of the leads. The positions of the atomic planes S_L and S_R , therefore, do not meet the asymptotic limit criterium as it is formally required by the scattering approach. However, since the current through the structure is conserved, any position of the planes is suitable for the calculation of conductance. Thus, if S_L is placed somewhere in the scattering region we have to sum up all multiple scattering contributions. All contributions in direction of the current cause \mathcal{T}^+ , whereas all multiple scattering contributions in opposite direction of the current give rise to \mathcal{T}^- . In the region of the lead where the potential is a small perturbation with respect to the bulk potential the contribution to the conductance due to \mathcal{T}^- is one order of magnitude smaller than \mathcal{T}^+ . To identify the transmission probabilities of individual eigenchannels the spectrums of the operators \mathcal{T}^+ and \mathcal{T}^- are arranged in a proper way using the symmetry analysis of eigenvectors. For further details we refer to Ref. 31.

Most of the structures studied in this work obey the C_{4v} symmetry determined by the fcc (001) surface (Fig.1). Further we denote individual channels by the

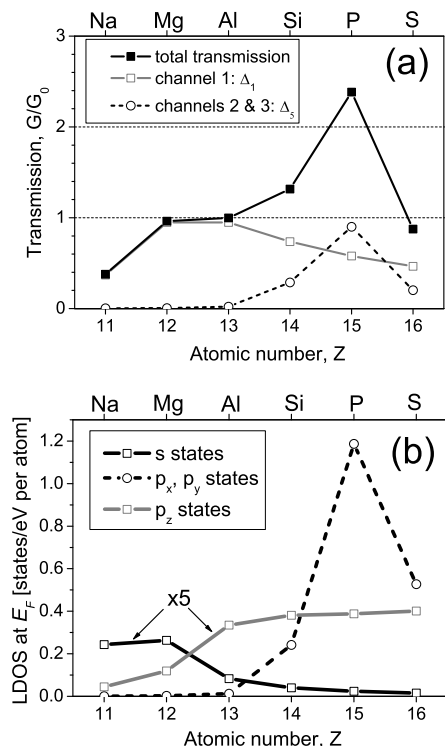


FIG. 2: Top panel (a): conductance and corresponding eigenchannel decomposition through the atomic chains with sp impurities connected to the Cu leads [see Fig.1(a)]. Bottom panel (b): Symmetry resolved LDOS at impurity sites, at the Fermi energy, *vs* atomic number of impurity.

indices of the irreducible representations of this group using notations of Ref. 32, common in the band theory. In addition, each channel can be classified according to the angular momentum contributions when the wave function of the channel is projected on the contact atom of the constriction. This is very helpful since the channel transmission can be related to the states of the contact atom.⁶ For example, the identity representation Δ_1 of the C_{4v} group is compatible with the s , p_z and d_{z^2} orbitals (here z is the axis perpendicular to the surface), while the two-dimensional representation Δ_5 is compatible with the p_x , p_y , d_{xz} , d_{yz} orbitals.

III. RESULTS AND DISCUSSION

A. Conductance through sp atoms

We consider first atomic constrictions shown in Fig.1a which are simulated by the straight three atom chains suspended between copper leads with different impurities in the center of the junction. The calculated conductance value of a pure Cu nanocontact is $0.96 G_0$. Only one channel contributes to the total transmission, it has Δ_1 symmetry and is projected on s and p_z orbitals of the

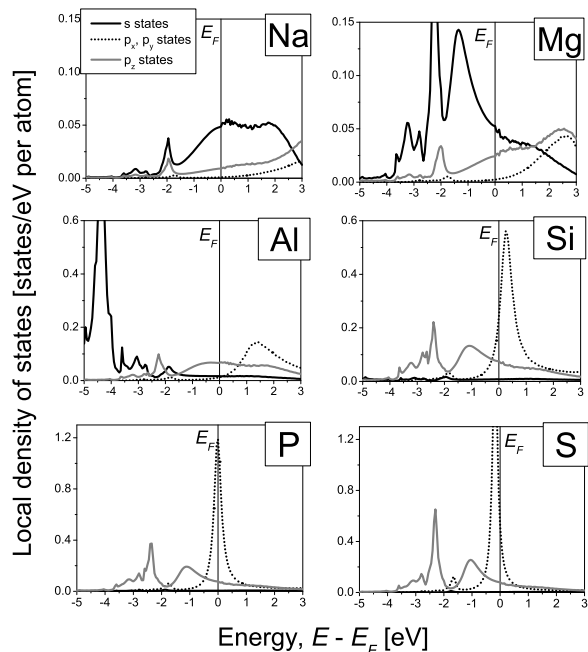


FIG. 3: Symmetry resolved LDOS at impurity atoms placed at the contact site of Cu junction [see Fig.1(a)].

contact Cu atom. In addition, small contributions from states with higher angular momentum (d_{z^2} and f_{z^3}) are also present. This result is in agreement with other theoretical studies^{7,9} as well as with experiments for noble metals.^{33,34}

We proceed with the discussion of the conducting properties of single sp atoms ($Z = 11 \dots 16$) attached to Cu electrodes (Fig.1a). In Fig.2 (top panel) we present the conductance together with the eigenchannel decomposition and compare it with the symmetry projected local density of states (LDOS) at the impurity atom, at the Fermi energy (bottom panel). We observe from Fig.2a that the conductance changes significantly depending on the type of sp impurity bridging the Cu leads. For example, conductance through the sodium atom is smaller than $0.5 G_0$ while in case of phosphorus it reaches a value of $2.4 G_0$. Our calculations show that three channels are involved in conductance: one sp_z -channel of Δ_1 symmetry and a double degenerate channel of Δ_5 symmetry which locally consists of p_x , p_y states when projection on the contact atom is performed. From Fig.2 we see that the variation of the eigenchannels transmission with atomic number follows the changes in the orbital resolved LDOS at E_F .

In case of Na, Mg and Al the transmission is essentially determined by one highly symmetric Δ_1 channel (Fig.2a). For sodium the electronic states at E_F have mainly s character (Fig.3) but transmission is small because of weak coupling to the Cu leads. As we move up to Mg and Al the s states are filled up with more electrons. At the same time, the p_z states contribute significantly to

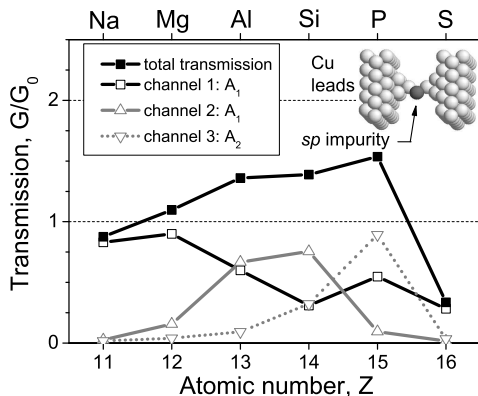


FIG. 4: Conductance and its eigenchannel decomposition for the zig-zag atomic chains suspended between the Cu leads with sp atoms placed at the contact site.

the LDOS at E_F (Fig.3). That causes a saturation of the Δ_1 channel transmission. For larger atomic numbers the Δ_1 channel is determined by p_z states only. The transmission of the Δ_1 channel is reduced again since for Si, P and S impurities the s states are occupied. The results of the calculations shown in Figs. 2 and 3 reveal that the increase of conductance through Si, P and S impurities is due to a virtual bound state formed by p_x and p_y orbitals (dashed line in Fig.3). This state gives rise to a double degenerate Δ_5 channel. The $p_x p_y$ resonance, which is situated just above E_F for Si, is pinned to the Fermi level in case of P, therefore the Δ_5 channel becomes highly open. For the S impurity the virtual bound state is occupied and the transmission of the Δ_5 channel drops.

To investigate the effect of atomic rearrangements on conductance we moved the sp atom from its symmetric position. The nanocontact is now simulated by a zig-zag-like chain suspended between Cu leads where the chain is a continuation of the fcc structure along the [001] direction (we show the exact geometry in the insert of Fig.4). The behavior of the conductance *vs* the atomic number (Fig.4) is similar to the previous case: transmission is smaller than 1.0 for Na, has a maximum for P and drops down for S. However, the absolute values are different for the two considered configurations. We found that the conductance consists again of three channels. Since the symmetry is reduced all channels are different and the degeneracy is lost. The 1st and 2nd channels correspond to an identity representation (A_g) of the S_2 group, while the 3rd channel is an antisymmetric one (A_u).

B. Conductance through 3d atoms attached to Cu leads

As we have seen, when atomic orbitals are present at the Fermi level they support additional conducting channels. That should be also true for the case of 3d transition metal impurities. They have five localized d states

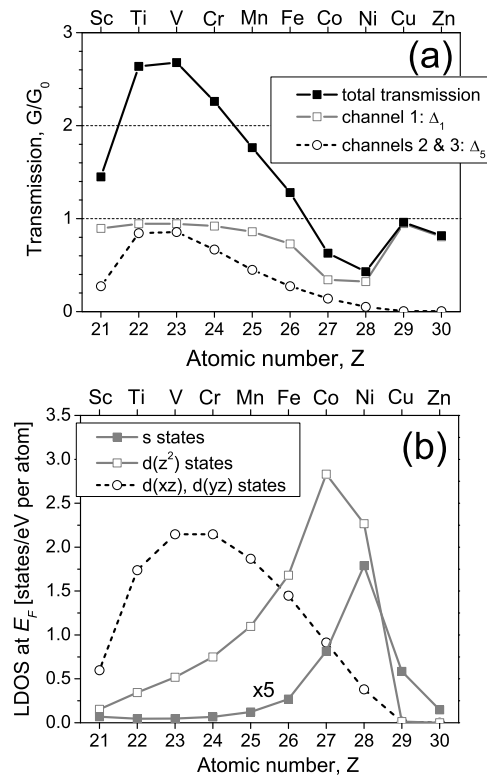


FIG. 5: Top panel (a): conductance and corresponding eigenchannel decomposition through the atomic chains with 3d impurities connected to the Cu leads [see Fig.1(a)]. Bottom panel (b): Symmetry resolved LDOS at impurity sites, at the Fermi energy, *vs* atomic number of impurity.

nearby E_F which potentially might be involved in the formation of new channels and the conductance could change as compared with $\approx 1.0 G_0$ found for a Cu constriction. Our results for the conductance of the systems with 3d transition metal impurities are given in Fig.5. We consider a single atom contact modelled by a short atomic chain connecting the Cu leads, with impurity inside the chain (Fig.1a). Indeed, we see that conductance varies in a broad range along the 3d series reaching values of about $2.7 G_0$ for Ti and V, and decreasing to $0.5 G_0$ in the case of a Ni atom. We have excluded many body effects (e.g., Kondo effect) from the consideration. As an approximation in the calculations the 3d impurities were supposed to have zero magnetic moments. That could be justified by the fact that at $T = 0$ the magnetic moment of the impurity is effectively screened by the conduction electrons.

Conductance is found to be a sum of three channels with Δ_1 and Δ_5 symmetry, where the last channel is two fold degenerate. To understand the behavior of channels transmission (Fig.5a) we present in Fig.5b the symmetry projected LDOS at the 3d impurities at the Fermi energy, as well as in the vicinity of E_F , for selected atoms (Fig.6). Calculations show that the LDOS nearby E_F is formed due to 4s and 3d states of transition metal atoms while 4p

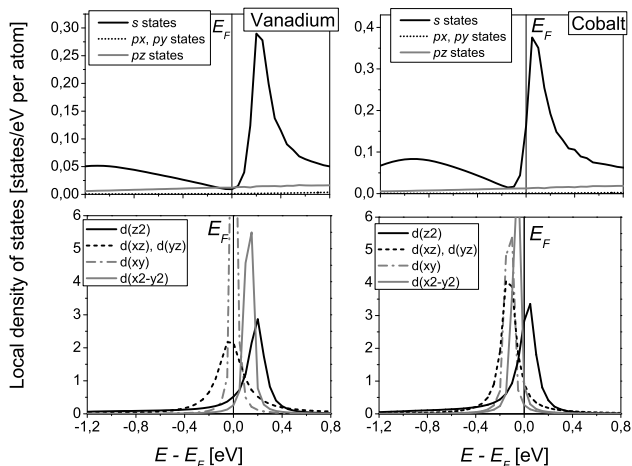


FIG. 6: Symmetry resolved LDOS at impurity atoms placed at the contact site of Cu junction [see Fig.1(a)].

states are above E_F and thus play no role for transport. As for $3d$ states, they form sharp resonances localized in the energy window of 1 eV around the Fermi level (Fig.6, low panels). The d_{xy} and $d_{x^2-y^2}$ resonance states, even if they are situated at the Fermi level, do not support open channels. Since the d_{xy} and $d_{x^2-y^2}$ orbitals are localized perpendicular to the wire axis effective coupling to the neighboring atoms is prevented. Consequently, the corresponding resonances look like sharp peaks in the LDOS (Fig.6, down panels).

Consider first the Δ_5 channel which is projected on

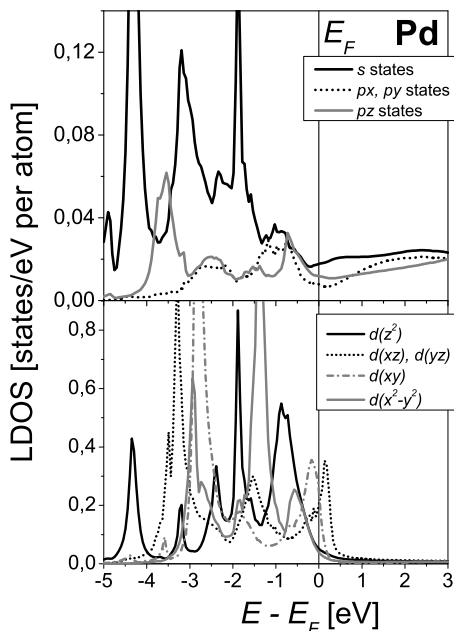


FIG. 7: Symmetry resolved LDOS at the central atom of the Pd junction shown in Fig.1(b).

d_{xz} , d_{yz} states. The two-fold degenerate resonance state of this symmetry is situated above E_F in case of Sc that leads to a relatively small transmission of the corresponding channel. When more d electrons are present at the contact atom, the d states move to lower energies. In particular, for Ti, V and Cr the d_{xz} , d_{yz} impurity state is situated very close to the Fermi level (Fig.6, down left panel) and causes high transmission of the Δ_5 channel. For larger atomic number the d_{xz} , d_{yz} resonance moves to energies below E_F and transmission of the corresponding channel is reduced.

The highly symmetric Δ_1 channel is open and is mainly due to s states for the first half of the $3d$ series, from Sc to Mn. The increase of the s and d_{z^2} LDOS in case of Fe, Co and Ni (Fig.5b) is accompanied by a reduction of the transmission. That is, because of the hybridization between s states and the d_{z^2} resonance (Fig.6, down right panel) with Δ_1 symmetry, the wave function becomes more localized at the impurity atom. From another point of view, the Δ_1 channel is scattered at the d_{z^2} impurity state. For Cu and Zn the d states are shifted to energies far below E_F , so that only a single s -channel is left.

C. Pd constrictions with transition metal impurities

One could expect a variety of different eigenchannels for atomic constrictions made of transition metals. An example of such a system is a Pd pyramid like contact shown in Fig.1(b), with conductance being $2.8G_0$. The LDOS at the contact atom is mainly d -like nearby the Fermi energy, as it is seen from Fig.7. This is also the case for the Pd surface. Since d states of different symmetry are available at the Fermi energy (Fig.7), six channels give a main contribution to conductance. These are one channel of Δ_1 symmetry: $\tau_1 = 0.72$ (sp_z -like); two double generate channels of Δ_5 symmetry: $\tau_2 = \tau_2' = 0.58$ (d_{xz} , d_{yz} -like) and $\tau_3 = \tau_3' = 0.32$ (p_x , p_y -like); and one

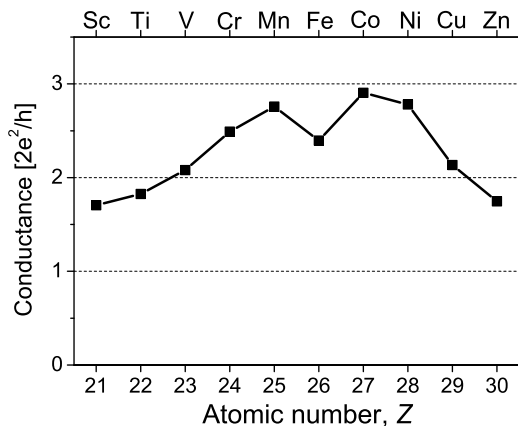


FIG. 8: Conductance through Pd pyramid-like junction contaminated by $3d$ impurities [see Fig.1(b)].

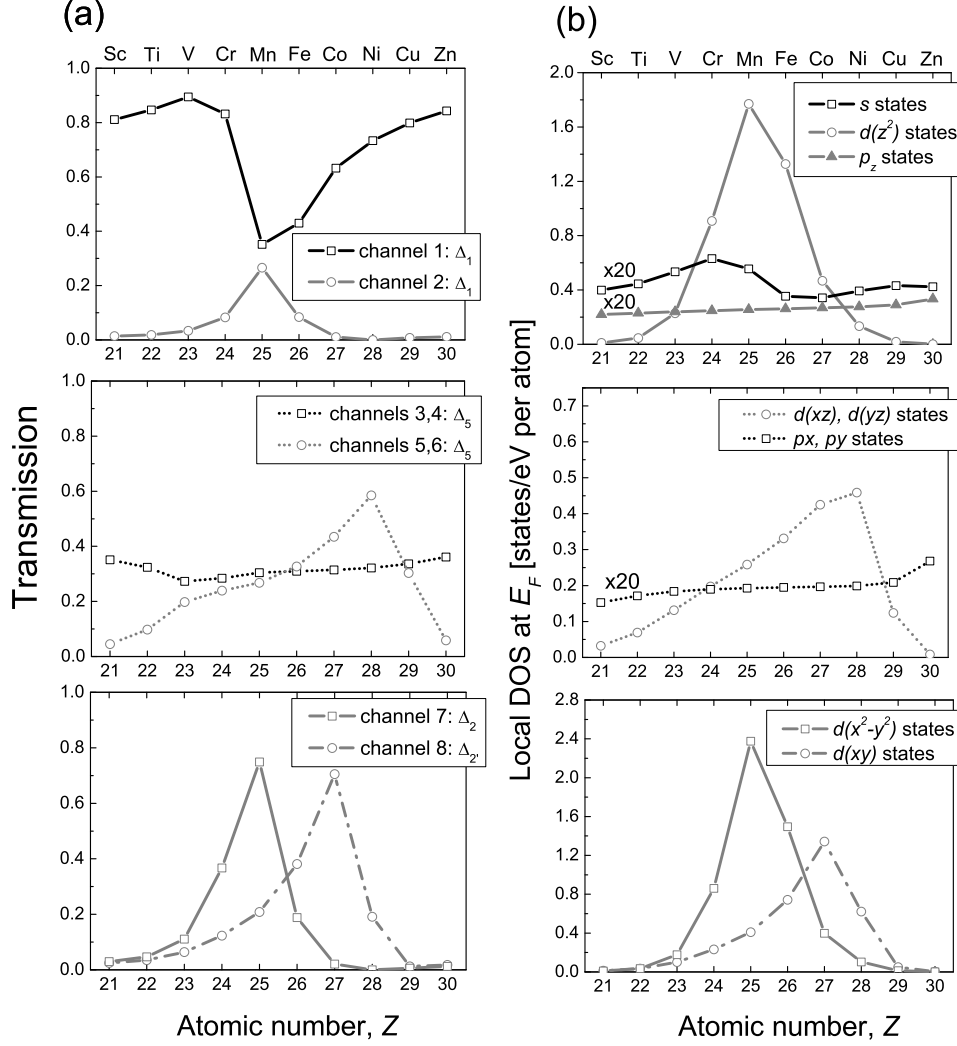


FIG. 9: (a) Left column: transmission probabilities of eigenchannels through Pd junctions contaminated by $3d$ impurities; (b) Right column: symmetry resolved LDOS at impurity atoms.

channel of Δ_2' symmetry, $\tau_4 = 0.24$ (d_{xy} -like). We would like to mention, that the channel with the highest symmetry (Δ_1) has the largest transmission. Here, the irreducible representations belong to the C_{4v} group.

Let us now study a situation where the contact atom of the otherwise Pd junction is substituted by $3d$ transition metal impurities. The conductance variation along the $3d$ series is shown in Fig.8. We observe that a Ni impurity does not affect conductance value of $2.8G_0$ of a Pd contact simply because Ni is isovalent to Pd. For other impurities conductance changes from $1.7G_0$ in case of Sc and Zn, up to $2.9G_0$ in the case of a Co atom. Eight channels give rise to the total transmission. Results of the individual transmission probabilities are presented in Fig.9 (left column) together with the LDOS at E_F projected on the corresponding orbitals of the impurity atoms (right column). Note, that due to a larger opening angle as compared with the first atomic configuration shown in Fig.1, the channels of Δ_2' (d_{xy}) and Δ_2 ($d_{x^2-y^2}$) symmetry contribute significantly to conductance, while they were closed in the case of the Cu constrictions with $3d$ impurities discussed in the previous section.

Without showing a detailed structure of the LDOS nearby the Fermi energy, we mention that a high density at E_F of the d states of different symmetry is always related to resonance-like states (see e.g. Fig.7 for the Pd atom). When some of these resonances approach the Fermi level, the transmission of the corresponding channel reaches a maximum. Such a situation takes place for the Δ_5 channel (d_{xz}, d_{yz} -like) in case of Ni (Fig.9, middle panels), as well as for the Δ_2 ($d_{x^2-y^2}$) and Δ_2' (d_{xy}) channels in case of Mn and Co, respectively (Fig.9, lower panels). For pure d channels mentioned above, a clear correlation between the partial LDOS at E_F and the transmission probabilities is observed. The other channel of Δ_5 symmetry does not show a strong variation of the transmission *vs* the atomic number of the impurity. This channel is mainly the p_x, p_y -like.

Finally, we note that two different channels of Δ_1 symmetry exhibit an interesting variation. One of them is sp_z -like, it is open at the beginning and at the end of the $3d$ series (Fig.9, upper panels). The d_{z^2} resonance approaching the Fermi level in case of Mn and Fe impurities acts in two ways. Firstly, due to a hybridization

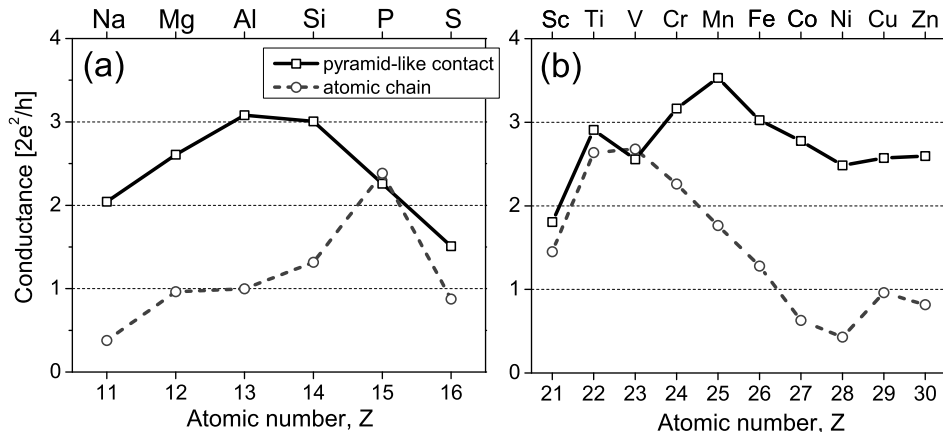


FIG. 10: Conductance through sp (left plot) and $3d$ (right plot) transition metal atoms attached to Cu leads in a different way as shown in Fig.1. Solid line: pyramid-like configuration (Fig.1b), dashed line: atomic chain (Fig.1a). The influence of the electrode material on the conductance can be seen if we compare solid line in plot (b) with results of Fig.8, where a geometry of the constriction was not changed but Pd was used instead of Cu.

with the s state it reduces the transmission of the already existing sp_z channel (that is similar to the case discussed in the previous section, Fig.5). Secondly, the d_{z^2} resonance itself opens a new channel of Δ_1 symmetry, which consequently is the d -like. Its transmission follows the variation of the d_{z^2} -LDOS when the atomic number is changed.

D. Does an atom possess certain conductance?

We have learnt from presented examples that conductance properties of individual atoms can be analyzed in detail with help of eigenchannel analysis. Therefore the question arises: can we attribute definite conductance to the particular atom? Comparing transmission through $3d$ transition metal impurities attached to Cu and Pd leads (Fig.5a and Fig.8, respectively), we see that the answer to this question is in general negative. This statement is also confirmed by results presented in Fig.10, where we compare transmission through sp and $3d$ transition metal atoms attached to Cu electrodes in a different way as it is shown in Fig.1. We have mentioned in the previous section, that due to a larger opening angle for the incident waves, conductance of pyramid-like constrictions increases as compared to nanocontacts simulated by atomic chains. The number of non-vanishing conducting channels needed to describe the conductance along sp and $3d$ series becomes also larger. Without going deep into details, we point out that number of eigenmodes increases up to 4 in case of sp impurities (Fig.10a) and up to 6 in case $3d$ transition metal atoms (Fig.10b). In particular, in the latter case, because of the increased coordination number of the contact atom, the d channels of $\Delta_{2'}$ (d_{xy}) and Δ_2 ($d_{x^2-y^2}$) symmetry become open for Ti and Mn, respectively. These channels were closed in the case of a nanocontact modelled by a three atom chain (see section III.B for discussion). Thus, the presented analysis gives no evidence to attribute a precise value of conductance to the given atom. A conclusion is that the

conductance is sensitive to the geometry of atomic constriction as well as to the type of electrodes. However, our results show that for the specified single-atomic contact eigenchannels can always be related to the electronic states of the appropriate symmetry at the Fermi energy.

IV. SUMMARY

In conclusion, based on the KKR Green's function method combined with the Kubo approach we have performed parameter-free *ab initio* calculations of the ballistic conductance through single sp and $3d$ transition metal atoms attached to Cu and Pd leads. We have investigated in which way the valency of the atom bridging two metallic leads is responsible for the number of conducting channels. We have found that both the chemical valency of the atom and the opening angle of the atomic constriction determine the number of eigenmodes. In accordance with the known tight-binding model by Cuevas *et al.*,⁶ we have confirmed by our study that the symmetry of the open conducting channels is related to the symmetry of the electronic states at the contact site. That allows to relate the open channels to the orbitals of the contact atom available at the Fermi energy. Furthermore, we have shown that impurity resonances approaching the Fermi level can open new channels of the appropriate symmetry. On the other hand, in some cases, the transmission of the existing channels can even be blocked by scattering at virtual bound states which have in this case the symmetry compatible with the symmetry of the open channels.

Acknowledgment

This work was supported by the Deutsche Forschungsgemeinschaft (DFG), Schwerpunktprogramm 1165 "Nanodrähte und Nanoröhren".

-
- ¹ H. Ohnishi, Yu. Kondo, and K. Takayanagi, *Nature* **395**, 780 (1998).
- ² C. J. Muller, J. M. van Ruitenbeek, and L. J. de Jongh, *Physica C* **191**, 485 (1992).
- ³ C. J. Muller, J. M. van Ruitenbeek, and L. J. de Jongh, *Phys. Rev. Lett.* **69**, 140 (1992); J. M. van Ruitenbeek, *Naturwissenschaften* **88**, 59 (2001).
- ⁴ N. D. Lang, *Phys. Rev. Lett.* **79**, 1357 (1997); N. D. Lang, *Phys. Rev. B* **55**, 9364 (1997).
- ⁵ N. Kobayashi, M. Brandbyge and M. Tsukada, *Jpn. J. Appl. Phys.* **38**, 336 (1999); N. Kobayashi, M. Brandbyge and M. Tsukada, *Phys. Rev. B* **62**, 8430 (2000); N. Kobayashi, M. Aono, and M. Tsukada, *Phys. Rev. B* **64**, 121402 (2001).
- ⁶ J. C. Cuevas, A. Levy Yeyati, and A. Martín-Rodero, *Phys. Rev. Lett.* **80**, 1066 (1998).
- ⁷ M. Brandbyge, N. Kobayashi, and M. Tsukada, *Phys. Rev. B* **60**, 17064 (1999).
- ⁸ A. Nakamura, M. Brandbyge, L. B. Hansen, and K. W. Jacobsen, *Phys. Rev. Lett.* **82**, 1538 (1999); K. S. Thygesen, M. V. Bollinger, and K. W. Jacobsen, *Phys. Rev. B* **67**, 115404 (2003); P. Jelínek, R. Pérez, J. Ortega, and F. Flores, *Phys. Rev. B* **68**, 085403 (2003); Y. Fujimoto and K. Hirose, *Phys. Rev. B* **67**, 195315 (2003); P. A. Khomyakov and G. Brocks, *Phys. Rev. B* **70**, 195402 (2004).
- ⁹ M. Brandbyge, J.-L. Mozos, P. Ordejón, J. Taylor, and K. Stokbro, *Phys. Rev. B* **65**, 165401 (2002); H. Mehrez, A. Wlasenko, B. Larade, J. Taylor, and P. Grütter, H. Guo, *Phys. Rev. B* **65**, 195419 (2002).
- ¹⁰ Ya. M. Blanter and M. Büttiker, *Physics Reports* **336**, 1 (2000); M. Büttiker, *Phys. Rev. B* **46**, 12485 (1992); M. Büttiker, *Phys. Rev. Lett.* **57**, 1761 (1986); M. Büttiker, Y. Ymry, R. Landauer, and S. Pinhals, *Phys. Rev. B* **31**, 6207 (1985).
- ¹¹ B. Ludoph, M. H. Devoret, D. Esteve, C. Urbina, and J. M. van Ruitenbeek, *Phys. Rev. Lett.* **82**, 1530 (1999).
- ¹² H. E. van den Brom and J. M. van Ruitenbeek, *Phys. Rev. Lett.* **82**, 1526 (1999); R. Cron, M. F. Goffman, D. Esteve, and C. Urbina, *Phys. Rev. Lett.* **86**, 4104 (2001).
- ¹³ R. Cron, E. Vecino, M. H. Devoret, D. Esteve, P. Joyez, A. Levy Yeyati, A. Martín-Rodero, and C. Urbina, *Dynamical Coulomb blockade in quantum point contacts*. In T. Martin, G. Montambaux, and J. Trân Thanh Vân, editors, *Electronic Correlations: from Meso- to Nano-Physics*, pages 17-22, Les Ulis, France, (2001). EDP Sciences.
- ¹⁴ M. Goffman, R. Cron, A. Levy Yeyati, P. Joyez, M. H. Devoret, D. Esteve, and C. Urbina, *Phys. Rev. Lett.* **85**, 170 (2000).
- ¹⁵ E. Scheer, P. Joyez, D. Esteve, C. Urbina, M. H. Devoret, *Phys. Rev. Lett.* **78**, 3535 (1997).
- ¹⁶ E. Scheer, N. Agraït, J. C. Cuevas, A. Levy Yeyati, B. Ludoph, A. Martín-Rodero, G. Rubio Bollinger, J. M. van Ruitenbeek, and C. Urbina, *Nature* **394**, 154 (1998).
- ¹⁷ R. Zeller, P. H. Dederichs, B. Ujfalussy, L. Szunyogh and P. Weinberger, *Phys. Rev. B* **52**, 8807 (1995); R. Zeller, *Phys. Rev. B* **55**, 9400 (1997).
- ¹⁸ H. U. Baranger and A. D. Stone, *Phys. Rev. B* **40**, 8169 (1989).
- ¹⁹ A. Enomoto, S. Kurokawa, and A. Sakai, *Phys. Rev. B* **65**, 125410 (2002); A. Enomoto, J. Mizobata, S. Kurokawa, and A. Sakai, *Surf. Sci.* **514**, 182 (2002).
- ²⁰ J. W. T. Heemskerk, Y. Noat, D. J. Bakker, J. M. van Ruitenbeek, B. J. Thijsse, and P. Klaver, *Phys. Rev. B* **67**, 115416 (2003).
- ²¹ N. Papanikolaou, A. Bagrets, and I. Mertig, *J. Phys.: Conf. Series*, **10**, 109 (2005).
- ²² N. D. Lang, *Phys. Rev. B* **52**, 5335 (1995).
- ²³ K. Hirose, N. Kobayashi, and M. Tsukada, *Phys. Rev. B* **69**, 245412 (2004).
- ²⁴ K. Palotás, B. Lazarovits, L. Szunyogh, and P. Weinberger, *Phys. Rev. B* **70**, 134421 (2004);
- ²⁵ J. K. Gimzewski and R. Möller, *Physica B*, **36**, 1284 (1987).
- ²⁶ N. Papanikolaou, R. Zeller, and P. H. Dederichs, *J. Phys.: Condens. Matter* **14**, 2799 (2002).
- ²⁷ S. H. Vosko, L. Wilk, and N. Nusair, *Can. J. Phys.* **58**, 1200 (1980).
- ²⁸ D. D. Koelling and B. N. Harmon, *J. Phys. C: Solid State Phys.* **10**, 3107 (1977).
- ²⁹ I. Turek, V. Drchal, J. Kudrnovský, M. Šob, and P. Weinberger, *Electronic Structure of Disordered Alloys, Surfaces and Interfaces* (Kluwer Academic, Boston, 1997).
- ³⁰ Ph. Mavropoulos, N. Papanikolaou, and P. H. Dederichs, *Phys. Rev. B*, **69**, 125104 (2004).
- ³¹ A. Bagrets, N. Papanikolaou, and I. Mertig, arXiv: cond-mat/0510073.
- ³² L. P. Bouckaert, R. Smoluchowski, and E. Wigner, *Phys. Rev.* **50**, 58 (1936)
- ³³ B. Ludoph and J. M. van Ruitenbeek, *Phys. Rev. B* **61**, 2273 (2000).
- ³⁴ A. I. Yanson, PhD thesis, Universiteit Leiden, The Netherlands (2001)